Bull Volcanol (2004) 66:381–391
DOI 10.1007/s00445-003-0319-5

RESEARCH ARTICLE

Tracy K. P. Gregg · Laszlo P. Keszthelyi

The emplacement of pahoehoe toes: field observations and comparison to laboratory simulations

Received: 21 March 2003 / Accepted: 28 August 2003 / Published online: 23 April 2004

Abstract We observed active pahoehoe lobes erupted on Kilauea during May-June 1996, and found a range of emplacement styles associated with variations in local effusion rate, flow velocity, and strain rate. These emplacement styles were documented and quantified for comparison with earlier laboratory experiments.

At the lowest effusion rates, velocities, and strain rates, smooth-surfaced lobes were emplaced via swelling, where new crust formed along an incandescent lip at the front of the lobe and the rest of the lobe was covered with a dark crust. At higher effusion rates, strain rates and velocities, lobes were emplaced through tearing or cracking. Tearing was characterized by ripping of the ductile crust near the initial breakout point, and most of the lobe surface was incandescent during its emplacement. This mechanism was observed to generate both smooth-surfaced lobes, and, when the lava encountered an obstacle, folded lobes. Cracking lobes were similar to those emplaced via tearing, but involved breaking of a thicker, brittle crust at the initial breakout of the lobe and therefore required somewhat higher flow rates than did tearing. Cracking lobes typically formed ropy folds in the center of the lobe, and smooth margins. At the highest effusion rates, strain rates, and flow velocities, the lava formed open channels with distinct levees.

The final lobe morphologies were compared to results from laboratory simulations, which were designed to infer effusion rate from final flow morphology, to quantitatively test the laboratory results on the scale of individual natural pahoehoe lobes. There is general agreement between results from laboratory simulations and natural lavas on the scale of individual pahoehoe lobes, but there are disparities between laboratory flows and lava flows on the scale of an entire pahoehoe lava flow field.

Editorial responsibility: A. Woods

T. K. P. Gregg (✉)
Dept. of Geology, 876 Natural Sciences Complex,
University at Buffalo,
PO Box 3050, Buffalo, NY 14260–3050, USA
e-mail: tgregg@geology.buffalo.edu
Tel.: (716) 645-6800 x 2463

L. P. Keszthelyi
Lunar and Planetary Laboratory,
University of Arizona,
Tucson, AZ 85712, USA

Present address:
L. P. Keszthelyi, United States Geological Survey,
2255 N Gemini Drive, Flagstaff, AZ 86001, USA

Introduction

The objective of this paper is to compare laboratory models of lava flow emplacement with field observations of active pahoehoe toes. Pahoehoe lava, characterized by interconnected lobes or buds with smooth or folded surfaces, is a common flow morphology that can be found in almost every basaltic province, from Earth's mid-ocean ridges to the surfaces of other planets (e.g., Fornari and Embley, 1995; Self et al., 1997; Keszthelyi et al., 1999). Despite their abundance, relatively little quantitative work has been done to interpret or predict the behavior of pahoehoe flows (Fink and Fletcher, 1978; Mattox et al., 1993; Hon et al., 1994; Crown and Baloga, 1999), probably because their advance is more chaotic than that of channeled lavas. Our ultimate goal is to constrain eruption and emplacement processes, based on the morphology of the final flow, for lavas that were erupted prehistorically or in remote regions where they were not observed while active. Since 1986, the ongoing Kilauea eruption has been dominated by tube-fed pahoehoe flows (Heliker and Wright, 1991; Heliker et al., 1998; Kauahikaua et al., 1998), providing excellent opportunities for quantitative observations of active pahoehoe lavas.

The overall morphology of pahoehoe flows is usually complex: a 10-m^2-patch of pahoehoe lava may contain several lobes of various dimensions with smooth, folded, and channeled surfaces (Gregg et al., 1997; Crown et al., 1998; Byrnes and Crown, 2001). These features yield information about local emplacement conditions on this

areal scale and corresponding timescales of minutes to hours. Although larger morphologic features, such as tumuli, provide emplacement constraints on larger and longer scales (Walker, 1991; Hon et al., 1994), they have no direct bearing on the behavior of the individual advancing lobes that characterize the emplacement of a pahoehoe flow. It is the morphology of the 1–10 m scale pahoehoe toes that record the (local) rate of advance of the flow.

Fink and others (Fink and Griffiths, 1990, 1992; Griffiths and Fink, 1992a and 1992b; Gregg and Fink, 1995, 1996, 2000) used a series of laboratory simulations to quantify the effusion rates of basaltic lava on the basis of final flow morphology. Each simulation was associated with a single dimensionless value, called Ψ, which incorporates the key physical parameters of both the extrusion and its environment (see section on "Laboratory Simulations" for more detailed explanations). By correlating laboratory morphologies with those of natural lava flows, they were able to assign a range of Ψ values to natural flows, and use that information to constrain the effusion rate of the lavas. However, none of these studies specifically examined subaerial pahoehoe flows. The inherent complexity of subaerial pahoehoe lava flows suggests that it may be difficult to assign a single morphologic type, and therefore a single range of Ψ, to an entire pahoehoe flow. Instead, the appropriate Ψ values may only be applicable to finite portions of a pahoehoe flow, reflecting the inherent variations during the emplacement of the flow field.

We have observed a range of morphologies in the active Hawaiian subaerial pahoehoe lava flow fields, including smooth, folded, and channeled lobes, emplaced via a continuum of different mechanisms. These morphologies are only a subset of lava types called "pahoehoe," but include the most common pahoehoe forms. Careful measurements of these active pahoehoe flow types, allow us to compare their Ψ values with those of laboratory morphologies and their associated Ψ values. As predicted by Fink and Griffiths (1990, 1992) and Griffiths and Fink (1992a, 1992b), results obtained from laboratory simulations can be used to constrain different types of pahoehoe lava flow emplacement, although there are some interesting complications encountered in the natural world.

Laboratory Simulations

Fink and others (Fink and Griffiths, 1990, 1992; Griffiths and Fink, 1992a, 1992b; Gregg, 1995; Gregg and Fink, 1995, 1996, 2000) used scaled laboratory simulations, in which polyethylene glycol (PEG) wax was extruded at a constant rate and temperature into a tank filled with cold sucrose solution, to quantitatively relate eruption parameters with final flow morphologies. By systematically varying effusion rate and cooling rate (controlled through PEG eruption temperature and ambient temperature), they repeatedly produced a sequence of 4 flow morphologies: pillowed, rifted, folded and leveed. Pillowed flows were generated at the lowest effusion rates and highest cooling rates. As effusion rate increased, and cooling rates decreased, pillowed flows gave way to rifted and folded flows. Leveed flows formed at the highest effusion rates and lowest cooling rates. Each of these flow types could be quantified using Ψ, a single dimensionless parameter that is essentially a ratio between the amount of time required for solidification of the flow surface to the time needed for heat to be advected through a distance equivalent to the flow depth. Ψ is defined as:

$$\Psi = \left(\frac{g\Delta p}{\eta}\right)^{3/4} Q^{1/4}\, t_s \text{ pointsource} \tag{1a}$$

$$\Psi = \left(\frac{g\Delta p}{\eta}\right)^{2/3} q^{1/3}\, t_s \text{ linesource} \tag{1b}$$

in which g is gravitational acceleration (m s^{-2}); $\Delta\rho$ is the difference between the fluid density and air density (kg m^{-3}); η is dynamic fluid viscosity (Pa s); Q is volumetric effusion rate (m^3 s^{-1}); q is linear effusion rate (m^2 s^{-1} m^{-1}); and t_s is the time required for the surface of the fluid to reach its solidus temperature (Griffiths and Fink, 1992a, 1992b). Fink and Griffiths (1990) derived this scaling relation by relating the amount of heat advected within a viscous flow and the amount of heat lost from the flow; for a detailed description of the derivation of Ψ see Fink and Griffiths (1990).

An error in the spreadsheet resulted in their initial publication of incorrect Ψ values (Fink and Griffiths, 1990); the corrected values are presented in Gregg and Fink (1996, 2000). Fink and Griffiths (1990) determined that laboratory pillowed flows (morphologically similar to submarine pillowed flows and to subaerial pahoehoe flows) formed at the highest cooling rates and lowest effusion rates, associated with $\Psi<0.65$. Rifted flows, in which plates of solid wax are separated by zones of liquid wax, along which spreading occurs, have $0.65<\Psi\leq 2.8$. Folded flows in the laboratory are similar to ropy pahoehoe lavas found in Hawaii, and have associated Ψ values of $2.8<\Psi\leq 6.4$. At the highest effusion rates and lowest cooling rates, leveed flows form, in which only the flow margins solidify, with $\Psi>6.4$. Gregg and Fink (2000) point out that these Ψ values marking morphologic transitions are valid only for flows emplaced on a smooth (i.e., allowing slip at the flow base) floors, and are therefore not directly applicable to natural lavas emplaced on relatively rough, "no-slip" surfaces. Gregg and Fink (2000) performed a series of similar experiments but instead emplaced the PEG onto a wire mesh that prevented slip at the flow base. Although Gregg and Fink (2000) produced the same sequence of four flow morphologies, they obtained the following transitional Ψ values for simulations emplaced on underlying slopes $\leq 10°$: pillows have $\Psi\leq 3$; rifts occur when $3<\Psi\leq 13$; folds form when $13<\Psi\leq 30$; and leveed flows are associated with $\Psi>30$ (coincidentally, these values are remarkably close to those originally published by Fink and Griffiths [1990] and

Griffiths and Fink [1992a, 1992b]). These transitional Ψ values are higher because a greater effusion rate is required to overcome frictional effects at the flow base, and are therefore better analogs to natural lava flows.

Gregg and Fink (2000) examined the role of underlying slope on PEG flow morphology by performing simulations on slopes ranging from 1–60°. They could not determine a straightforward way to quantitatively incorporate underlying slope into the Ψ values associated with each flow. However, they concluded that as underlying slope increased (up to 40°), folded and leveed flows appeared with eruption conditions (effusion rate and cooling rate) that generated rifted or pillowed flows at lower slopes. In other words, increasing underlying slope had an effect similar to that of increasing effusion rate. At underlying slopes $\geq$40°, leveed flows were formed at almost all effusion rates and cooling rates; Gregg and Fink (2000) interpreted these results to indicate that at the steepest slopes, gravitational forces began to dominate the flow regime. Recent experimentation to quantify the tensile strength of solid PEG for comparison with solid basalt suggest that PEG is 2–3 orders of magnitude stronger than basalt (Soule and Cashman, 2004). Gregg and Smith (2003) suggest that this difference in tensile strengths may be responsible for the predominance of simulated leveed flows on slopes $\geq$40°. These results also suggest that directly relating underlying slope in the laboratory to underlying slope in the real world may be complex. However, at low slopes (<10°) these effects are not pronounced in the laboratory (Gregg and Fink, 2000) and so results from shallow-sloping experiments can most likely be more directly applied to natural flows emplaced on slopes <10°.

In all the simulations referred to above, eruption parameters (effusion rate, eruption temperature, eruption viscosity and ambient temperature) were kept constant during the course of the experiment. Thus, each PEG flow developed a single, dominant flow morphology. In the natural world, a lava flow can typically be characterized by a single morphology if the scale is also specified (e.g., the entire flow, or a single flow lobe).

Fink and Griffiths (1990) related Ψ values to effusion rate and lava viscosity for a number of well-constrained subaerial eruptions and demonstrated that the natural lavas have associated Ψ values that correspond well with the observed final lava flow morphology. However, the effusion rates used in their calculations are typically "average" values: that is, the total eruptive volume divided by the entire eruption duration. Effusion rate commonly changes during the course of an eruption (e.g., Wadge, 1977 and 1981; Cas and Wright, 1987; Stasuik et al., 1993), causing the Ψ value calculated for the eruption to change with time. Similarly, local variations in effusion rate at the same moment would result in spatial variations in Ψ; for example, lava spilling out of a channel and flowing over a levee advances at a slower rate than lava contained within the channel (e.g., Pinkerton and Sparks, 1978; Jurado-Chichay and Rowland, 1995). Furthermore, active pahoehoe flows display a range of morphologies, ranging from smooth and folded toes tens of centimeters in diameter to lava channels hundreds of meters long which, according to Fink and Griffiths (1990), should be associated with distinct Ψ values. In other words, spatial and temporal variations in Ψ for a natural lava flow strongly suggest that careful measurements of active pahoehoe lavas are required to quantitatively compare laboratory results with these natural lavas.

Field Observations

The gross morphologic category of "pahoehoe" covers a multitude of disparate lava expressions, ranging from the classic billowy or ropy surfaces to lava types transitional to a'a, such as slab and spiney pahoehoe (Dutton, 1884; Einarsson, 1949; Macdonald, 1953; Wentworth and Macdonald, 1953; Swanson, 1973; Rowland and Walker, 1987). We confine our discussions to "classic" pahoehoe toes, which are characterized by a continuous, flexible skin during emplacement. Within the confines of "classic" pahoehoe, we observed three types of flow lobe surfaces: smooth, folded, and channeled (Fig. 1). In this study, we define a lava lobe as a pod or bud of lava that is being fed from an identified and discrete source (typically another lobe). We also observed the two distinct mechanisms of lobe emplacement described in Keszthelyi and Denlinger (1996), which are distinguished by whether incandescent lava is exposed at the front or at the back of an advancing lobe. It is interesting to note that smooth lobes can be formed by either mechanism and that the latter mode of emplacement can form any of the three surface morphologies. This can seriously complicate attempts to decipher the style of emplacement of frozen pahoehoe lava flows.

In this paper we will call the lobes that have the thinnest crust at the front swelling lobes (Fig. 2a). These swelling lobes, with incandescent lava at the advancing tip, form at the lowest local effusion rates. The outer carapace of chilled lava does not advance, though it does expand laterally as it is stretched by inflation. The lobe envelops or engulfs obstacles, almost invariably producing a smooth upper surface irrespective of the scale of the underlying roughness. The slowest moving lobes are apparently very sensitive to cooling rate: they display a strong tendency to hug the nearby recently emplaced warm lobes instead of boldly advancing over new cold ground, possibly because they are unable to advance more than a few centimeters over a cold substrate before freezing. Also, because the liquid is confined within a relatively stiff skin, significant pressure may build up within the lobe, allowing it to advance uphill (Fig. 3),although we have not observed any lobes to climb above the elevation of their initial breakout point. This strongly argues against significant overpressurization within most pahoehoe lobes on a length scale larger than a few meters. Swelling lobes tend to be only a few tens of centimeters in diameter, although they may be more than 3–5 m long.

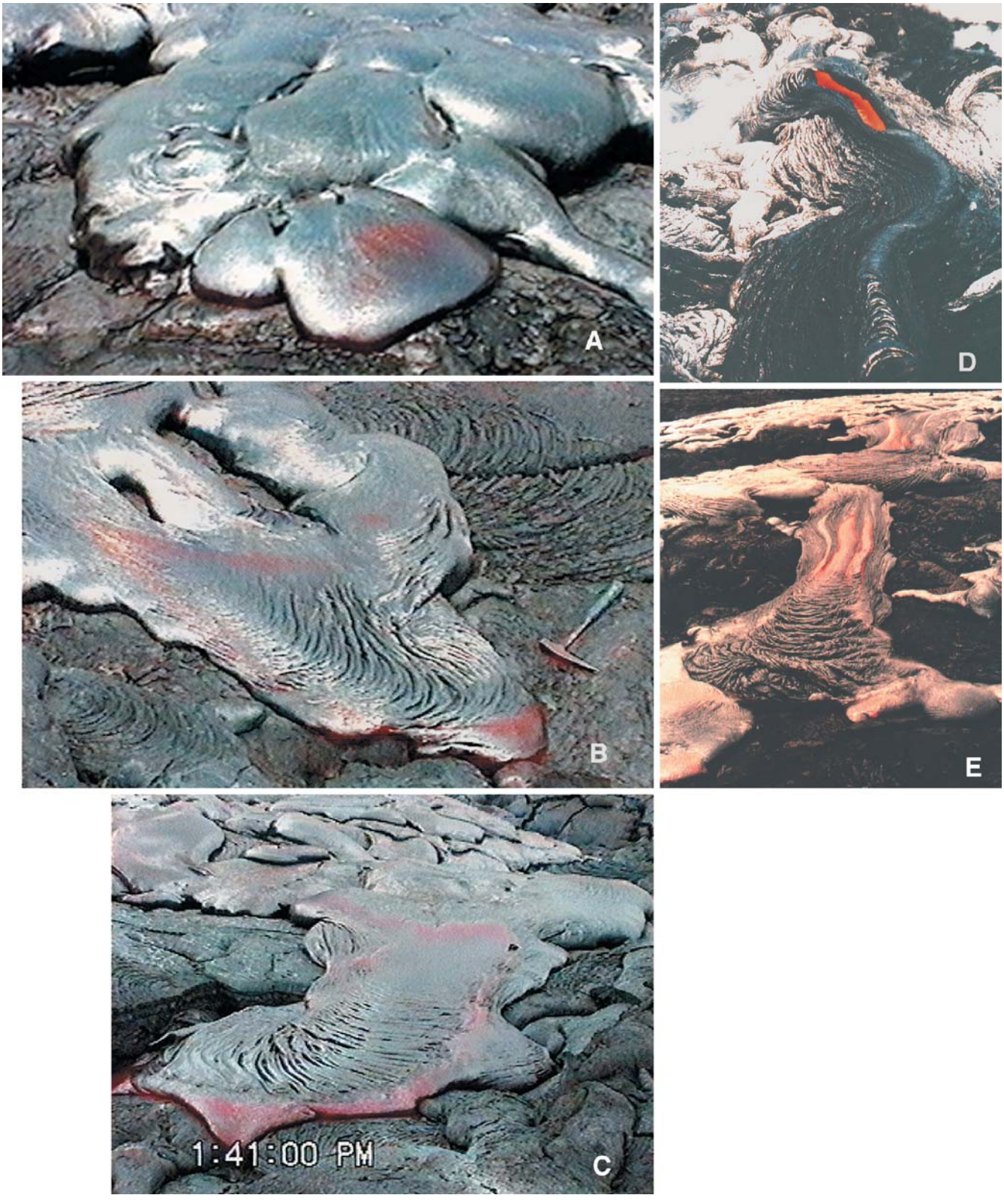

Fig 1 Pahoehoe lobe morphologies (*a*) Smooth-surfaced lobe being emplaced in the "tearing" mode (*b*) 1-m-long, ropy lobe being emplaced in the tearing mode over earlier smooth lobes in center of photo. Active smooth-surfaced swelling lobe advances over earlier lobes in upper left corner of photo (*c*) 3–4-m long cracking lobes with surfaces transitional between ropy and channeled. Lobe in foreground feeds multiple smooth-surfaced tearing lobes (*d*) 1-m-wide channeled lobe roofing over. Note flow-parallel "ropes" related to levee formation, not compression (*e*) 3-m-wide partially roofed channeled lobe. All photos from USGS, taken in 1996 on Kilauea by L Keszthelyi

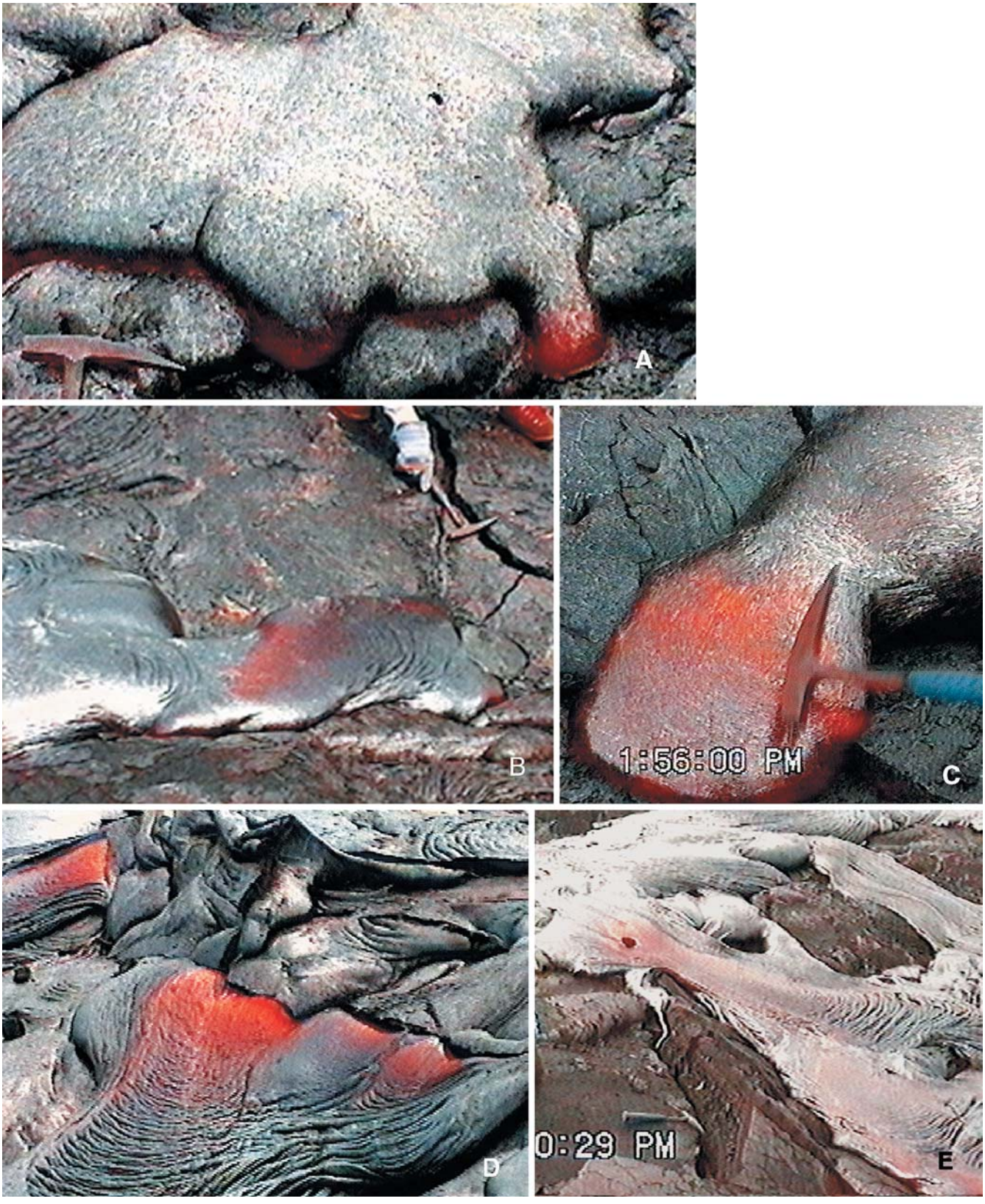

Fig 2 Pahoehoe emplacement styles (*a*) 2-m-wide, 30-cm-long swelling lobe with incandescent lip and smooth surface (*b*) 20 – 40-cm long ropy and smooth-surfaced tearing lobes (*c*) 3-m-wide smooth-surfaced tearing lobe (*d*) 3-m-wide ropy-surfaced cracking lobe (*e*) 2-m-wide open-channel lobe splitting around an obstacle

Fig 3 Climbing (and drooping) pahoehoe lobe 50-cm-long swelling lobe with tip that climbed 8–10 cm

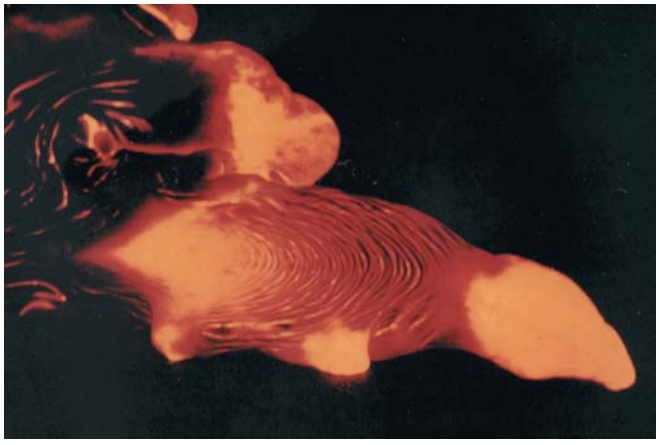

Fig 4 Night photograph showing crust forming on a cracking lobe. Note that only a small triangular incandescent area (with apex pointed upflow) remains as this >50-cm-long cracking lobe crusts over. Smaller, smooth-surfaced, swelling lobes are leaking out from the length of the ropy margins of the main lobe

In contrast, lobes that have the thinnest crust at the point of initial breakout (upstream from the lobe tip) cover a range of dimensions from the smallest toes only a few tens of centimeters long to large, open-channel lobes over ten meters long and more than one meter wide. There are several points at which this continuum can be divided, and we will use the terms *tearing*, *cracking*, and *channeled* (Fig. 2b,c,d) to distinguish points along the continuum. Tearing toes are initiated by the ripping of the skin of an earlier lobe that is still sufficiently thin to be flexible, whereas cracking lobes breakout from beneath crust that has cooled to the point of being brittle. For the purposes of this study, we define a lobe as channeled if it develops levees and the lobe is longer than it is wide. In general, effusion rates and lobe volumes both increase as the regime changes from tearing to cracking to channeled. We reiterate that there is a continuum between the tearing and channeled lobes, but the changes in the mechanics of emplacement as a function of scale warrant the use of different words to describe both endmembers and an intermediate case. It is still useful to describe each individual style of lobe emplacement in some detail.

Higher effusion rates and the lack of a chilled crust at their breakout point characterize the continuum of tearing and cracking lobes. The skin that forms at the top of the lobe is often rolled over at the front in a caterpillar-tread fashion. When the tearing/channeled lobe meets an obstacle, the translating upper skin may buckle and fold, resulting in ropy pahoehoe (Fink and Fletcher, 1978; Gregg et al., 1997). Alternatively, the crust at the front of the lobe may eventually become too thick and strong to continue to advance and the upper skin starts to "pile-up", or imbricate. Thus, the front of a lobe may become an obstacle to its own procession and the presence of ropes is not necessarily diagnostic of a pre-existing topographic obstacle. As the skin grows by accretion at the flow front and by cooling from the sides, the exposed area of incandescent lava on the lobe surface shrinks (Fig. 4). After a solid crust has formed over the lobe, the continued flux of lava is accommodated by a combination of inflation and new breakouts. In many cases, the hardening front of a wide tearing or cracking lobe will feed a number of slower tearing or swelling lobes even before the top of the parent lobe has completely crusted over.

Larger open-channel lobes form at the highest effusion rates (>3000 $cm^3\ s^{-1}$) we observed (see Table 1) and share many of the characteristics of small cracking or tearing lobes. For example, the manner in which the solid crust grows over tearing and cracking lobes is essentially identical to the roofing over process of lava tubes as described in Peterson and Swanson (1974). However, the absolute size of open-channel lobes also leads to important differences; most prominent is the fact that larger channeled lobes are capable of transporting large pieces of solidified crust. This solid crust often leads to the concentration of shear along discrete, centimeter-scale zones between distinct crustal plates moving at different relative velocities, or between moving plates and the stationary flow margin (e.g., Pinkerton and Swanson, 1974; Pinkerton and Sparks, 1978). The velocity profile across such a channel surface is not that of a simple Newtonian or Bingham fluid (e.g., Cas and Wright, 1987), nor does it necessarily reflect the velocity profile of the moving lava beneath. If the crust remains sufficiently hot

Table 1 Emplacement parameters for subaerial pahoehoe lobes

Lobe type	Strain rate (ϵ_{xx}; s^{-1})	Flow velocity (v; cm s^{-1})	Effusion rate (Q; $m^3\ s^{-1}$)	Min Ψ	Nominal Ψ	Max Ψ
Swelling	10^{-4}	<1	$<6\times10^{-4}$	2.0	8.3	334
Tearing	10^{-3}	1–3	6×10^{-4}–2.4×10^{-3}	2.0–2.8	8.3–8.7	265–281
Cracking	10^{-2}	>3	$>3\times10^{-3}$	>3.0	>8.7	>281

and thin to deform in a ductile manner at the shear rate it is experiencing, surface folds may form where the lobe encounters obstacles. However, if the crust is relatively cooler and thicker, slab pahoehoe is generated where the flow top is slowed. Flow-parallel lineations (some with positive relief that make them look similar to flow-perpendicular folds) may appear as the flow levees grow inward (Fig 1d); these are not true "folds" as they are not associated with lateral compression (cf. Fink and Fletcher, 1978). The types of behavior seen in active pahoehoe lobes are reminiscent of some of the behavior seen in laboratory wax experiments (e.g., Gregg and Fink, 2000).

Kilauea Field Measurements

Kilauea volcano began its most recent period of activity in 1983, and has been erupting more or less continuously since then. An excellent review of the eruption activity can be found in Mattox et al. (1993). We have carefully observed and measured the emplacement of 14 active pahoehoe lobes during episode 53 of the Pu'u O'o—Kupaianaha eruption to obtain the data necessary to calculate Ψ for each lobe and determine if these Ψ values agree with those predicted from the laboratory simulations. Eqns. 1a, 1b show that the required parameters are density, viscosity, local effusion rate, and the rate of crust formation. Episode 53 was characterized by relatively constant effusion at the Pu'u O'o vent of 3–5 m^3/s, and tube-fed flows. Numerous tube breakouts near the shore provided safely accessible pahoehoe flows.

Lobe effusion rates were measured using both visual inspection and video recordings of active lavas on Kilauea during May-June, 1996. Flow velocities were obtained by filming the advance of a lava flow with a consistent scale (such as a rock hammer or tape measure) in the field of view, or by throwing rocks of known dimensions onto the surface of an advancing flow and tracing their downstream velocity. (Note that for channeled lobes, the flow-front velocity did not necessarily equal the velocity of the lava actively flowing within the channel center.) We estimated lobe thickness in situ and from video by comparing with a known scale or tape measure. In situ measurements were obtained using a tape-measure where possible; however the extreme heat of the flows makes these measurements only accurate to within ±3 cm. For slowly advancing lobes with lengths and widths on the scales of tens of centimeters to <2 m, we were able to place a rock hammer (with precisely known dimensions) in the field of view filmed by the video camera. This allowed us to obtain near-continuous measurements of lobe dimensions that we believe to be accurate to within 1–3 cm, depending on the total field of view of the video frame from which measurements were being made. Lobe widths $\geq$1.5 m were measured from the video using available scales (such as rock hammers or people); these measurements are accurate to ±5 cm because of the larger field of view required to obtain the measurements and possible perspective errors. Perspective problems were minimized both by carefully choosing the filming angle, and by assuring that objects of known size were present throughout the field of view. For example, a person would walk the length of the lobe within the field of view, or the rocks of known dimensions mentioned above were traced as they flowed downstream. Effusion rates were calculated by multiplying lobe width, thickness, and velocity. Strain rates were estimated from video images, by measuring the change in lobe width or length with time. All numbers given below were obtained from our field or video measurements.

Strain rates (ϵ_{xx}), flow velocities (v; the rate of advance of the lobe front or the velocity of the red-hot liquid portions of channeled lobes) and effusion rates (Q) for lobes emplaced by swelling, tearing or cracking are shown in Table 1. The one measured channeled lobe had a maximum in-channel flow velocity of 1.2 m s^{-1}, localized strain rates of 1–2 s^{-1} in the shear zones, and a total effusion rate of 16±10 m^3 s^{-1}. This large uncertainty in the effusion rate results from the difficulty in determining the depth of flow in a wide channel: we could only measure depth at the lobe margins with certainty. Because such channeled lobes represent the sudden release of lava accumulated over minutes to hours, it is not surprising that, for a brief time, the local effusion rate is higher than the total eruption rate (typically 3–5 m^3 s^{-1} during this period).

We collected several of the smooth toes, emplaced via swelling. They were sectioned with a rock saw and subjected to detailed petrographic examination . From this work and other samples collected previously, we observed that the lobes were ~50 vol% vesicles, corresponding to a bulk lava density of ~1400 kg m^{-3}. Determinations of the lava viscosity were also made using the chemistry of these (and similar) lobes and temperatures derived by both glass geothermometry and thermocouples. Using the technique of Shaw (1972) gives a lava viscosity of about 40 Pa s for the pure liquid phase. This viscosity must be then corrected for the solid and gas inclusions (i.e., crystals and bubbles) in the bulk fluid (e.g., Pinkerton and Stevenson, 1992). The Kilauea lavas observed and examined have <1 vol.% phenocrysts, so the effect of the solid phase can be ignored.

The effect of bubbles on the rheology of lavas is far more complicated than the effect of phenocrysts, particularly when they comprise 50 vol.% of the lava. At the low strain rates observed in the small swelling and tearing pahoehoe toes, it may be appropriate to assume that the bubbles do not deform extensively and can be treated as solid spheres, in which case their effect on viscosity would be similar to the effect of same-sized phenocrysts. This assumption is supported by the fact that the vesicles within these lobes are very round, although it is possible that they were deformed during lava emplacement and returned to spherical once the lava stopped flowing. The outermost <1-mm-thick rind on these lobes contains bubbles that are stretched by as much as a factor of 40 (Hon et al., 1994). Furthermore, at high strain rates, it is known that bubbles reduce the effective viscosity of liq-

uids (e.g., Manga, 1996). This is seen qualitatively by the observation that vesicular lavas provide less resistance to vigorous mechanical stirring than dense lavas (Keszthelyi and Self, 1998). Thus bubbles can increase or decrease the effective viscosity of the lava depending on the local strain rate, and the volumetric abundance of vesicles. Given the low strain rates in the active lobes we observed in 1996, and the high volume percentage (50 vol.%) of vesicles, we expect the bubbles to have increased the bulk viscosity of the flowing lava. This assumption may break down at the relatively high strain rates observed within the shear zones of channeled lobes.

Given these complications, we have used a range of viscosities from 10^2-10^4 Pa s for the lava viscosity: using Pinkerton and Stevenson's (1992) relations indicates that ~50 vol.% rigid bubbles would increase the bulk viscosity of Hawaiian lavas from 40 Pa s to about 3000–4000 Pa s. Our selected range is in general accord with other estimates of the bulk viscosity of Kilauea lavas (e.g., Shaw et al., 1968; Heslop et al., 1989). However, we note that methods that examine the behavior of the entire flow can give viscosities many orders of magnitude higher and a significant yield strength, especially for a'a flows (e.g., Fink and Zimbelman, 1986; Moore, 1987). Because we are interested in the bulk viscosity of the fluid lava, rather than the effective viscosity of the entire flow (which is probably dominated by the effect of the crust), these lower estimates are more appropriate for use in Eqs. 1a and 1b. The effect of viscosity on Ψ can be seen in Fig. 5. Viscosity is included in the calculation for Ψ (Eqs. 1a, 1b). Note that, for a given effusion rate, a runnier lava is associated with a higher Ψ value; this is consistent with laboratory observations. In other words, a runnier lava is more likely to generate a leveed flow at a given effusion rate while a more viscous flow is more likely to produce a pillowed or rifted flow. Similarly, increasing the effusion rate can have an effect similar to decreasing the viscosity, again consistent with laboratory observations (Fink and Griffiths, 1990; Gregg and Fink, 2000). The application of Ψ to natural lavas carries with it the assumption of Newtonian behavior for the fluid. Although the formation of a solid crust undoubtedly imparts a yield strength to the behavior of both natural and simulated flows, we believe that the morphologic and dynamic similarities between natural and simulated flows, coupled with the demonstrated applicability of Ψ-values to natural basalt flows (Fink and Griffiths, 1990; Griffiths and Fink, 1992a, 1992b; Gregg and Fink, 1995, 1996, 2000) shows that the non-Newtonian behavior of natural basalts can be neglected in the comparisons we make here.

Determining t_s, the "crust formation" timescale, in nature is also fraught with uncertainties, and is controlled largely by the choice of the lava solidification temperature (Fig. 6). Note that the longer the crust formation timescale (i.e., the longer it takes the surface crust to solidify), the more likely it is that channels will develop over pillows or rifts; this is consistent with both laboratory and field observations (Fink and Griffiths, 1990; Gregg and Fink, 2000). Fink and Griffiths (1990) equated

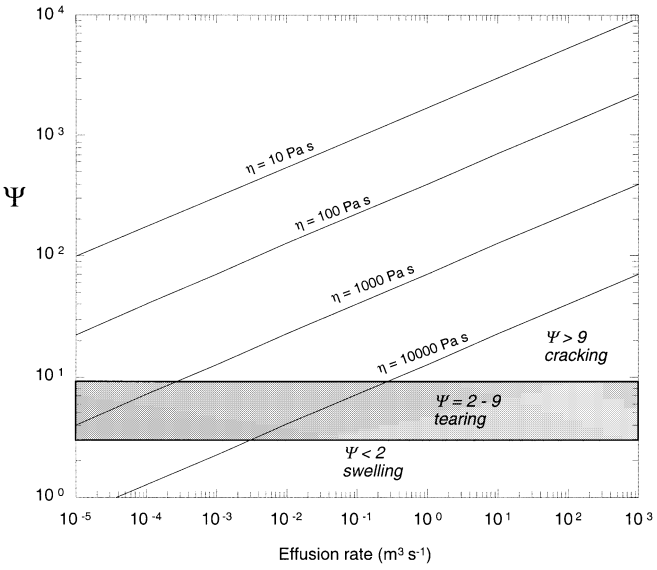

Fig 5 The effect of lava viscosity in the relation between volumetric effusion rate (Q) and Ψ. Calculations made using ρ_l = 1400 kg m^{-3} and t_s = 10 s. The regions identified as swelling, tearing and cracking are indicated by the boundaries of the *shaded area* (In the laboratory, the transition from pillows to lobes occurs at Ψ = 3). Note that as viscosity decreases, Ψ increases for a given effusion rate. This implies that a runnier, less-viscous lava is more likely to generate a leveed flow whereas a stickier, more-viscous lava is more likely to create a pillowed or rifted flow at the same eruption rate (Gregg and Fink, 2000). This is what is observed in laboratory simulations (Fink and Griffiths, 1990; Gregg and Fink, 2000)

t_s to the calculated time for the surface of the lava to drop below the glass transition temperature. However, the glass transition temperature (~725 °C for basalts [e.g., Ryan and Sammis, 1981; Fink and Griffiths, 1990]) is a thermodynamic concept related to the state of the metastable liquid quenched into the glass and has little direct relevance to the mechanical behavior of the lava. Instead, Kilauea lavas appear to transition from "liquid-like" behavior to more "solid-like" behavior around 1065–1070 °C (e.g., Shaw et al., 1968; Ryan and Sammis, 1981; Hon et al., 1994). In Hawaii, pahoehoe surfaces will drop from a typical initial temperature of 1150–1135 °C (Keszthelyi, 1996) to below 1000 °C in a second or less (Keszthelyi and Delinger, 1996).

We have decided to use a simple field criterion to define when a mechanical crust has formed. In the field, we would rest a standard rock hammer on its head on top of the lava, supporting it so that all the weight of the hammer was pressing into the lava surface. If there is no crust, a hammer thus pressed against the lobe will readily sink into the lava. In contrast, if a crust exists, a large portion of the surface of the lobe will bend or sag under gentle prodding but the hammer will not enter the hotter interior of the lobe. Of course, with sufficient force, it is possible to tear the crust and have the hammer penetrate into the liquid core. Our observations indicate that, by this definition, a mechanical crust forms after 11–12 seconds. However, on faster moving lobes, the continued stretch-

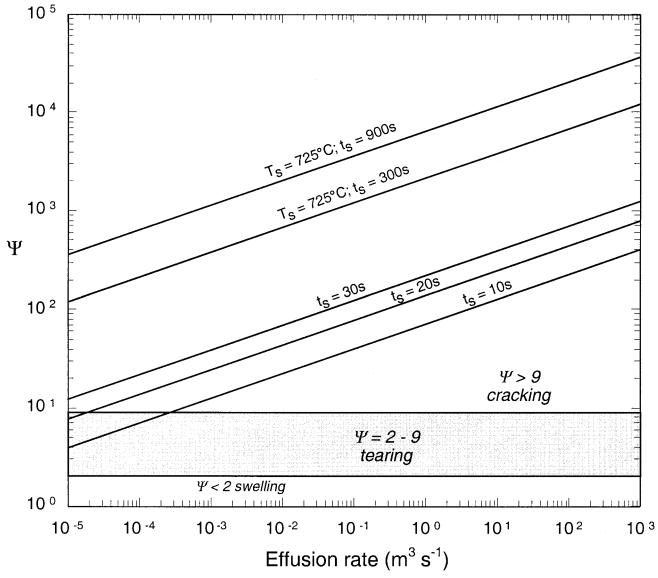

Fig 6 Relation between volumetric effusion rate (Q) and Ψ for different solidification times. The values for t_s (= 10, 20, 30 s) are based on field criteria and are therefore not associated with a specific temperature. The greater the solidification time, the farther the flow can advance prior to being crusted over, all other parameters being equal. Therefore, a longer solidification time results in an increased likelihood of the formation of leveed or folded flows over the generation of pillowed or rifted flows. This is consistent with qualitative laboratory observations (Fink and Griffiths, 1990 and Gregg and Fink, 2000). The range of Ψ values calculated from field data as corresponding with swelling, tearing, and cracking lobes are indicated by the boundaries of the *shaded region*

ing of the skin prevents its hardening for ~30 seconds. Although somewhat qualitative, these measurements were reproduced on multiple lobes by 4 different people. This time for mechanical crust formation was used for the value of t_s in Eqs. 1a and 1b to calculate Ψ-values for individual lobes.

Comparisons of field and laboratory values of Ψ

Table 1 lists the measurements and 3 estimates of Ψ values for each emplacement style. The lowest Ψ are calculated using a viscosity of 10^4 Pa s and crust formation after 10 s. The moderate case uses 3000 Pa s and 12 s, while maximum values are determined using 100 Pa s and 30 s. With increasing flow rate, we would expect the effective viscosity of the lava to decrease due to shear thinning and the crust formation time to increase. However, because increasing crust formation time also increases the rate of heat loss from the uncrusted flow (and therefore increasing viscosity) these two effects may effectively cancel each other.

Ψ values in the range between the minimum and nominal values in Table 1 are in good agreement with laboratory simulations, in spite of simplifying assumptions. Note, for example, that ignoring the increase in viscosity of the lava caused by the bubbles leads to Ψ values completely outside the range of those encountered in the laboratory experiments. The swelling lobes on Kilauea appear to generally correspond to pillows in the laboratory (Ψ<2–8 in the field and <3 in the lab). However, the distinction between rifted and folded wax flows at Ψ=13 is not obviously correlated to the change from tearing to cracking pahoehoe lobes at Ψ=3–9. This is not surprising because we measured the demarcation between different styles of *emplacement* of pahoehoe lobes, not their final morphologies. The change from tearing to cracking emplacement, for example, does not correspond to the change from rifting to folded surface morphologies; swelling emplacement forms only smooth, pillow-like lobes and open-channel lobe leaves recognizable channels after the flow has frozen. Still, because tearing lobes can produce folded surfaces, we would expect the Ψ value marking the transition from rifted to folded flows to be within the range of tearing lobes (e.g., Ψ=2–9) which is significantly less than the Ψ=13 value from laboratory simulations. The simplest explanation for this discrepancy is that the skin on basalt pahoehoe lobes is easier to fold than is the skin on wax flows. Folds on the wax flows are much larger, both in amplitude and wavelength, (relative to the thickness of the lobe) than the classic pahoehoe ropes (Gregg et al., 1997). Furthermore, the tensile strength of cold, solid PEG is approximately 2–3 orders of magnitude greater than the tensile strength of cold, solid basalt (Soule and Cashman, 2004). Although the process of surface folding does not appear to be directly related to the tensile strength of the material (Fink and Fletcher, 1978), the greater strength of the PEG would be consistent with its being relatively more difficult to fold.

While the comparison between Kilauea field data and laboratory simulations is quite good when examining individual lobes, it fails when considering the entire flow field. The total eruption rate *at the vent* through the bulk of episodes 51–55 of the ongoing Pu'u O'o eruption has been 3 and 5 m^3 s^{-1} (Heliker et al., 1998; Kauahikaua et al., 1998). Assuming ~50 vol.% bubbles, this corresponds to 6–10 m^3 s^{-1} for the purpose of our calculations and results in Ψ values of ~20, 60 and 2000 for the minimum, nominal and maximum cases, respectively (Keszthelyi, 1994). This would suggest that the current eruption should be forming mostly open channel flows instead of being dominated by pillow-like pahoehoe lobes: but only if all the lava exiting the vent is concentrated in a single surface flow.

This mismatch between the laboratory and field data points to a fundamental difference. We suggest that the key is that the laboratory simulations do not reflect the complexity of the lava transport system that feeds the front of pahoehoe flows. The pahoehoe lobes we studied were not fed directly from the eruptive vent, or even directly from the lava tube. Instead, they were fed from within a broad, sheet-like flow. In effect, the source for the pahoehoe lobes was not a point source, but a diffuse source along the active margin of the flow—typically tens of meters to a few hundred meters in length. Thus, the lava surface at any given location only preserves the *local*

effusion rate. To determine the total effusion rate, it is necessary to integrate over the length of the active flow margin. Unfortunately, for most inactive pahoehoe flow fields, their inherently compound nature makes it impossible to determine exactly how much of the field was active at any given time.

Therefore, results from the laboratory simulations may be most applicable to individual lobes rather than to entire flow fields. Fink and Griffiths (1990) compare the results of their laboratory experiments to natural lava flows and find the best agreements with those flows that are least complex; using Walker's (1972) definition, the laboratory simulations tend to generate *simple* flows and a pahoehoe flow field is a *compound* flow. For example, the 1984 Mauna Loa, Hawaii, flow can be modeled as a single, channeled lobe (e.g., Crisp et al., 1995; Sakimoto and Gregg, 2001), and there is good correlation between it and the laboratory simulations. Similarly, the various incarnations of the post-1980 Mount St. Helen's' dacite domes largely behaved as individual lobes or "pillows", and the behavior of these natural "pillows" is easily related to the behavior of laboratory pillowed flows because both are simple flows. In looking at a compound pahoehoe flow field, however, it is impossible to assign a single behavior or emplacement mechanism that is appropriate for the entire flow: the flow may be tube-fed with breakouts, for example, or it may be inflated with lava flowing from ruptured tumuli (Hon et al., 1994). Lava emplaced within a tube will obviously behave differently from lava being fed from a tube breakout.

This is why we believe that although the results from the laboratory simulations are applicable to the natural world, there are inherent limitations. These limitations are not scale-dependent, but process-dependent: it does not matter if the lobe is hundreds of meters across (e.g., Mount St. Helen's domes) or a few centimeters (a pahoehoe toe). Rather, it is significant that both these features were emplaced during a single, roughly continuous event.

Conclusions

We have found good correspondence between the behavior of active pahoehoe lobes on Kilauea volcano and wax flows in laboratory simulations. In general, the pillowed wax flows correspond with swelling pahoehoe lobes and form smooth surfaces; rifted and folded wax flows behave like tearing and cracking pahoehoe lobes and form both smooth and ropy surfaces; and both wax and pahoehoe form open channels at the highest flow rates and Ψ values.

However, laboratory and field data match only if we correct for the effect of bubbles on the effective lava viscosity and use field data to determine the time for the formation of a rheologically significant skin. We estimate that the bubbles in the Kilauea lavas increase its effective viscosity by a factor of ~100 from the bubble-free state.

We have now identified quantitative boundaries on the conditions that lead to different styles of pahoehoe lobe emplacement, and such constraints have important implications for understanding the general development of complex pahoehoe flows (cf. Crown and Baloga, 1998). However, there are at least two major difficulties in using the <10-m-scale surface morphology of a pahoehoe flow to determine eruption parameters. First, it is difficult to ascertain from the final morphology if the flow was emplaced in the swelling, tearing, or cracking mode. The latter two styles of emplacement can form both smooth and ropy surfaces, and also grade seamlessly into open-channel lobes. Second, the lobe morphology provides constraints only on the local effusion conditions. It is necessary to determine and examine all areas of a flow field that were active at any given time if one wishes to constrain parameters such as total eruption rate from resulting volcanic morphologies. This is particularly relevant in the study of submarine and extraterrestrial volcanic terranes, where available high-resolution imagery may cover only a small portion of a single volcanic flow field.

References

Byrnes JM, DA Crown (2001) Relationships between pahoehoe surface units, topography, and lava tubes at Mauna Ulu, Kilauea Volcano, Hawaii. J Geophys Res 106:2139–2151

Cas RAF, Wright JV, (1987) Volcanic Successions: Modern and Ancient, Allen & Unwin, London, 528 pp

Crisp J, Cashman KV, Bonini JA, Hougen SB, Pieri DC (1995) Crystallization history of the 1984 Mauna Loa lava flow. J Geophys Res 99:7177–7198

Crown DA, Baloga SM (1999) Pahoehoe toe dimensions, morphology, and branching relationships at Mauna Ulu, Kilauea Volcano, Hawaii. Bull Volcanol 61:288–305

Dutton CE (1884) Hawaiian volcanoes, US Geol Surv, 4th Ann Rept, p 75–219

Einarsson T 1949 The eruption of Hekla 1947–1948: IV, 3 The flowing lava Studies of its main physical and chemical properties Soc Scientarium Islandica, Reykjavik, 70 pp

Fink JH, Fletcher RC (1978) Ropy pahoehoe: Surface folding of a viscous fluid. J Volcanol Geotherm Res 4:141–170

Fink JH, Griffiths RW (1990) Radial spreading of viscous-gravity currents with solidifying crust. J Fluid Mech 221:485–509

Fink JH, RW Griffiths (1992) A laboratory analog study of the surface morphology of lava flows extruded from point and line sources. J Volcanol Geotherm Res 54:19–32

Fink JH, JR Zimbelman (1986) Rheology of the 1983 Royal Gardens basalt flows, Kilauea Volcano, Hawaii. Bull Volcanol 48:87–96

Fornari DJ, Embley RW (1995) Tectonic and volcanic controls on hydrothermal processes at the mid-ocean ridge: An overview based on near-bottom and submersible studies in Physical, Chemical, Biological, and Geological Interactions within Seafloor Hydrothermal Systems. In: Humphris S, Zierenberg R, Mullineaux L, Thomson R (eds) Amer Geophys Union Monograph 91:1–46

Gregg TKP, Fink JH (1995) Quantification of submarine lava-flow morphology through analog experiments. Geology 23:73–76

Gregg TKP, Fink JH (1996) Quantification of extraterrestrial lava flow effusion rates through laboratory simulations. J Geophys Res 101 16,891-16,900

Gregg TKP, Fink JH (2000) A laboratory investigation into the effects of slope on lava flow morphology. J Volcanol Geotherm Res 96:145–159

Gregg TKP (1995) Quantification of lava flow morphologies through analog experiments. PhD Thesis, Arizona State University, 112 pp

Gregg TKP, Fornari DJ, Kesztheyli LP (1997) Quantifying mid-ocean ridge eruption dynamics: Temporal and spatial variations in submarine lava flow emplacement processes. Geol Soc Amer Abstracts with Programs 29 A-138

Gregg TKP, Smith DK (2003) Volcanic investigations of the Puna Ridge, Hawaii: Relations of lava flow morphologies and underlying slopes J Volcanol Geotherm Res (in press)

Griffiths RW, Fink JH (1992a) Solidification and morphology of submarine lavas: A dependence on extrusion rate. J Geophys Res 97:19,729–19,737

Griffiths RW, Fink JH (1992b) The morphology of lava flows in planetary environments: Predictions from analog experiments. J Geophys Res 97:19,739–19,748

Heliker C, Wright TL (1991) The Pu'u O'o-Kupaianaha eruption of Kilauea. Eos Trans Amer Geophys Union 72:521

Heliker CC, Mangan MT, Mattox TN, Kauahikaua JP (1998) The Pu'u 'O'o Kupaianaha eruption of Kilauea, November 1991-February 1994: Field data and flow maps, U S Geological Survey, OF 98–0103, pp 10

Heslop SE, Wilson L, Pinkerton H, Head JW (1981) Dynamics of a confined lava flow on Kilauea Volcano, Hawaii. Bull Volcanol 51:415–432

Hon K, Kauahikaua J, Denlinger R, MacKay K (1994) Emplacement and inflation of pahoehoe sheet flows: Observations and measurements of active lava flows on Kilauea Volcano, Hawaii, Geol Soc Amer Bull 106:351–370

Jurado-Chichay Z, Rowland SK (1995) Channel overflows of the Pohue Bay flow, Mauna Loa, Hawaii: Examples of the contrast between surface and interior lava. Bull Volcanol 57:117–126

Kauahikaua J P, Cashman K V, Mattox TN, Heliker CC, Hon KA, Mangan MT, Thornber CR (1998) Observations on basaltic lava streams in tubes from Kilauea Volcanic, Island of Hawaii. J Geophys Res103:27,303–27,323

Kesztheyli LP (1994) Calculated effect of vesicles on the thermal properties of cooling basaltic lava flows. J Volcanol Geotherm Res 63:257–266

Keszthelyi L (1996) Measurements of the cooling of pahoehoe lava flows. Eos Trans AGU 77: F807 (abstract)

Kesztheyli LP, Delinger R (1996) The initial cooling of pahoehoe flow lobes. Bull Volcanol 58:5–23

Keszthelyi L, Self S (1998) Some physical requirements for the emplacement of long basaltic lava flows. J Geophys Res 103:27,447–27,464

Keszthelyi LP, Self S, Thordarson T (1999) Application of recent studies on the emplacement of basaltic lava flows to the Deccan Traps. In: Subbarao KV (ed) Deccan volcanic province, Memoir—Geological Society of India, 43, Part 1, pp 485–520

Macdonald GA (1953) Pahoehoe, aa, and block lava Am J Sci 251:169–191

Manga M (1996) Waves of bubbles in basaltic magmas and lavas. J Geophys Res 101:17,457–17,465

Mattox TN, Heliker C, Kauahikaua J, Hon K (1993) Development of the 1990 Kalapana flow field, Kilauea Volcano, Hawaii. Bull Volcanol 55:407–413

Moore HJ (1987) Preliminary estimates of the rheological properties of 1984 Mauna Loa lava. In: Decker RW, Wright TL, Stauffer PH (eds) Volcanism in Hawaii. US Geol Survey Prof Paper 1350:1569–1587

Peterson DW, Swanson DA (1974) Observed formation of lava tubes during 1970–71 at Kilauea Volcano, Hawaii. Stud Speleol 2:209–223

Pinkerton H, Stevenson RJ (1992) Methods of determining the rheological properties of magmas at sub-liquidus temperatures. J Volcanol Geotherm Res 53:47–66

Pinkerton H, Sparks RSJ (1978) Field measurements of the rheology of lava. Nature 276:383–385

Rowland SK, Walker GPL (1987) Toothpaste lava; characteristics and origin of a lava structural type transitional between pahoehoe and aa. Bull Volcanol 49: 631–641

Ryan MP, Sammis CG (1981) The glass transition in basalt. J Geophys Res 86:9519–9535

Sakimoto SEH, Gregg TKP (2001), Channeled flow: Analytic solutions, laboratory experiments, and applications to lava flows. J Geophys Res 106:8629

Self S, Thordarson T, Keszthelyi LP (1997) Emplacement of continental flood basalt lava flows. In: JJ Mahoney, Coffin MF (eds) Large igneous provinces: Continental, oceanic, and planetary flood volcanism. Geophysical Monograph 100:381–410

Shaw HR, Wright TL, Peck DL, Okamura R (1968) The viscosity of basaltic magma: An analysis of field measurements in Makaopuhi lava lake. Hawaii Am J Sci 226:225–264

Shaw HR (1972) Viscosities of magmatic silicate liquids: An empirical method of prediction. Am J Sci 272:870–893

Soule A, Cashman K (2004) The mechanical properties of solidified polyethylene glycol 600, an analog for lava crust. J Volcanol Geotherm Res 129:139–153

Stasuik MV, Jaupart C, Sparks RSJ (1993) Influence of cooling on lava -flow dynamics. Geology 21:335–338

Swanson DA (1973) Pahoehoe flows from the 1969–1971 Mauna Ulu eruption, Kilauea Volcano, Hawaii. Geol Soc Am Bull 84:615–626

Wadge G 1977 The storage and release of magma on Mt Etna J Volcanol Geotherm Res 2:361–384

Wadge G (1981) The variation of magma discharge during basaltic eruptions. J Volcanol Geotherm Res 11:139–168

Walker GPL (1972) Compound and simple lava flows and flood basalts, International Symposium on Deccan Trap and Other Flood Eruptions, Proceedings, Part I, Bull Volcanol 35:579–590

Walker George PL (1991) Structure, and origin by injection of lava under surface crust, of tumuli, "lava rises", "lava-rise pits", and "lava-inflation clefts" in Hawaii. Bull Volcanol 53:546–558

Wentworth CK, Macdonald GA (1953) Structures and forms of basaltic rocks in Hawaii. US Geol Surv Bull 994, 98 pp